WERE RNNS ALL WE NEEDED?

Anonymous authors
Paper under double-blind review

ABSTRACT

The scalability limitations of Transformers regarding sequence length have renewed interest in recurrent sequence models that are parallelizable during training. As a result, many novel recurrent architectures, such as S4, Mamba, and Aaren, have been proposed that achieve comparable performance. In this work, we revisit traditional recurrent neural networks (RNNs) from over a decade ago: LSTMs (1997) and GRUs (2014). While these models were slow due to requiring to backpropagate through time (BPTT), we show that by removing their hidden state dependencies from their input, forget, and update gates, LSTMs and GRUs no longer need to BPTT and can be efficiently trained in parallel. Building on this, we introduce minimal versions (minLSTMs and minGRUs) that (1) use significantly fewer parameters than their traditional counterparts and (2) are fully parallelizable during training ($175\times$ faster for a sequence of length 512). Lastly, we show that these stripped-down versions of decade-old RNNs match the empirical performance of recent sequence models.

1 INTRODUCTION

Over the past few years, Transformers (Vaswani et al., 2017) have been the dominant architecture in many areas, leading to advancements in tasks like machine translation (Devlin et al., 2019), text generation (Brown et al., 2020), and more. However, Transformers have a quadratic computational complexity in the sequence length, making them prohibitively expensive for long sequences, especially in low-resource settings. As such, numerous works have investigated the design of more efficient alternatives that achieve competitive performance with that of Transformers. Recently, there has been a renewed interest in recurrent sequence models that can be trained efficiently processing their context in parallel (Tiezzi et al., 2024a;b). These models (1) during training require only linear memory in the sequence length and (2) at inference time are rolled out recurrently token-by-token, requiring only constant memory. As a result, these models can scale to significantly longer sequences than Transformers[1].

A family of efficiently trainable recurrent sequence models that has recently gained much traction is that of state-space models, specifically the recently proposed Mamba (Gu & Dao, 2024). Mamba (S6) is a state-space model that differentiates itself from prior works by leveraging input-dependent transitions. The recent success of Mamba and the proposals of many new variants of state-space models has led to several survey papers (Wang et al., 2024; Patro & Agneeswaran, 2024; Qu et al., 2024). Another extensively explored group of methods is those based on attention. Peng et al. (2023) proposed a linear attention model that can be written recurrently while being trained in parallel. Feng et al. (2024) showed that softmax attention (and Transformers) can be viewed as a recurrent neural network (RNN). Building on their RNN formulation of attention, they proposed Aaren, a softmax attention model, that can be computed in parallel for efficient training or unrolled sequentially as an RNN for efficient inference. Although many recurrent models have been proposed with vastly different architectures, these recent state-of-the-art methods are all efficiently trainable using the same algorithm – the parallel prefix scan algorithm (Blelloch, 1990).

Inspired by the striking algorithmic similarities between the numerous recently proposed sequence models, we revisit LSTMs (Hochreiter & Schmidhuber, 1997) and GRUs (Cho et al., 2014) from a modern lens. As traditional RNNs from over a decade ago, LSTMs and GRUs are only computable sequentially and require to backpropagate through time (BPTT) during training. As such, LSTMs

[1]The title of this paper pays tribute to the original Transformers paper, "Attention is All You Need".

and GRUs were far too slow to scale beyond a few hundred tokens, resulting in their deprecation. Revisiting these models, we show that by removing hidden state dependencies from their input, forget, and update gates, LSTMs and GRUs no longer need to BPTT and can be trained efficiently using the parallel scan algorithm. Building on this, we simplify LSTMs and GRUs further by removing their constraints on output range, (i.e., their use of $\tanh$) and ensuring their output is time-independent in scale. These steps result in minimal versions (minLSTMs and minGRUs) that (1) use significantly fewer parameters than their traditional counterpart and (2) are trainable in parallel ($175\times$ faster for a context length of 512). Finally, we show that these stripped-down versions of decade-old RNNs match the empirical performance of modern recurrent sequence models, challenging the prevailing trend in the community toward increasing architectural and algorithmic complexity.

2 Background

In this section, we review recurrent neural networks (RNNs). RNNs are recurrent sequence models that maintain a hidden state across time steps, capturing temporal dependencies. As such, RNNs are particularly suitable for sequence modelling settings such as those involving time series, natural language processing, and other sequential tasks where context from previous steps informs the current prediction. Vanilla RNNs (Elman, 1990), however, struggle with issues of vanishing and exploding gradients, limiting their ability to learn long-term dependencies.

2.1 LSTM

Addressing this limitation, Hochreiter & Schmidhuber (1997) introduced Long Short-Term Memory (LSTM) networks. LSTMs are enhanced RNNs designed to mitigate the vanishing gradient problem, allowing the model to learn long-term dependencies. LSTMs are computed as follows:

$$\begin{aligned}
\boldsymbol{f}_t &= \sigma(\mathrm{Linear}_{d_h}([\boldsymbol{x}_t, \boldsymbol{h}_{t-1}])) \\
\boldsymbol{i}_t &= \sigma(\mathrm{Linear}_{d_h}([\boldsymbol{x}_t, \boldsymbol{h}_{t-1}])) \\
\tilde{\boldsymbol{c}}_t &= \tanh(\mathrm{Linear}_{d_h}([\boldsymbol{x}_t, \boldsymbol{h}_{t-1}])) \\
\boldsymbol{o}_t &= \sigma(\mathrm{Linear}_{d_h}([\boldsymbol{x}_t, \boldsymbol{h}_{t-1}])) \\
\boldsymbol{c}_t &= \boldsymbol{f}_t \odot \boldsymbol{c}_{t-1} + \boldsymbol{i}_t \odot \tilde{\boldsymbol{c}}_t \\
\boldsymbol{h}_t &= \boldsymbol{o}_t \odot \tanh(\boldsymbol{c}_t)
\end{aligned}$$

where $\odot$ represents an element-wise multiplication of vectors, t is the current timestep, $\boldsymbol{h}_t$ is the outputted hidden state, $[\boldsymbol{x}_t, \boldsymbol{h}_{t-1}]$ represents the concatenation of $\boldsymbol{x}_t$ with $\boldsymbol{h}_{t-1}$, d_h is the size of the hidden state, $\boldsymbol{c}_t$ is a cell state that maintains information over the sequence, and $\tilde{\boldsymbol{c}}_t$ is the candidate cell state to be added, $\boldsymbol{i}_t$, $\boldsymbol{f}_t$, and $\boldsymbol{o}_t$ are gating mechanisms. The input gate $\boldsymbol{i}_t$ controls how much new information from the candidate cell state is added. The forget gate $\boldsymbol{f}_t$ determines the proportion of information in the cell gate to discard. The output gate $\boldsymbol{o}_t$ decides what information from the cell state should be outputted. The σ and $\tanh$ are used for scaling to ensure that the output does not explode/vanish. An LSTM module maintains both a cell and a hidden state and, in total, contains $O(4d_h(d_x + d_h))$ parameters.

2.2 GRU

Simplifying LSTM, Cho et al. (2014) introduced Gated Recurrent Unit (GRU) which only uses two gates and a single state instead of LSTM's three gates and two states (hidden and cell state). GRU's reduced complexity leads to faster training and inference times while achieving competitive performance in many tasks. GRUs are computed as follows:

$$\begin{aligned}
\boldsymbol{z}_t &= \sigma(\mathrm{Linear}_d([\boldsymbol{x}_t, \boldsymbol{h}_{t-1}])) \\
\boldsymbol{r}_t &= \sigma(\mathrm{Linear}_d([\boldsymbol{x}_t, \boldsymbol{h}_{t-1}])) \\
\tilde{\boldsymbol{h}}_t &= \tanh(\mathrm{Linear}_d([\boldsymbol{x}_t, \boldsymbol{r}_t \odot \boldsymbol{h}_{t-1}])) \\
\boldsymbol{h}_t &= (1 - \boldsymbol{z}_t) \odot \boldsymbol{h}_{t-1} + \boldsymbol{z}_t \odot \tilde{\boldsymbol{h}}_t
\end{aligned}$$

where $\tilde{\boldsymbol{h}}_t$ is the candidate hidden state that represents a potential new value for the hidden state. GRU combines LSTM's forget and input gates into a single update gate $\boldsymbol{z}_t \in (0, 1)$ which decides how much of the past information to carry forward (i.e., $1 - \boldsymbol{z}_t$) and how much new information from the candidate hidden state to add (i.e., $\boldsymbol{z}_t$). Additionally, LSTM's output gate is removed and instead, a reset gate $\boldsymbol{r}_t$ is added that controls how much past information is used in computing the candidate hidden state. GRU reduces the total number of parameters and computations, requiring only $O(3d_h(d_x + d_h))$ parameters. However, GRUs and LSTMs are only computable sequentially. As a result, during training they require backpropagating their gradients through time (BPTT), requiring linear training time and greatly limiting their ability to scale to long contexts.

2.3 Parallel Scan

Due to this limitation, Transformers replaced LSTMs and GRUs as the defacto sequence modelling method for years by leveraging parallelization during training. However, Transformers have a quadratic complexity in the sequence length, limiting their ability to scale to long contexts. Recently, a resurgence of many new recurrent models have been proposed as replacements for Transformers that achieve comparable performance and are trainable in parallel, while avoiding the BPTT issue that traditional RNNs (e.g., LSTMs and GRUs) faced. Although many different architectures have been proposed, many of these models are efficiently trained using the parallel prefix scan algorithm (Blelloch, 1990).

The parallel scan algorithm is a parallel computation method for computing N prefix computations from N sequential data points via an associative operator $\oplus$ (e.g., $+$ and $\times$). The algorithm efficiently computes $\{\bigoplus_{i=1}^{k} u_i\}_{k=1}^{N}$ from $\{u_k\}_{k=1}^{N}$. In particular, we can apply the parallel scan method for efficiently computing a popular family of functions: $v_t = a_t v_{t-1} + b_t$ where $v_t, a_t, b_t \in \mathbb{R}$ and $v_0 \leftarrow b_0$ (Martin & Cundy, 2018; Heinsen, 2023). The method takes as input $a_1, \ldots, a_n$ and $b_0, b_1, \ldots, b_n$ and computes via parallel scans $v_1, \ldots, v_n$.

3 Methodology

Naturally, the aforementioned algorithm also extends to vectors: $\boldsymbol{v}_t = \boldsymbol{a}_t \odot \boldsymbol{v}_{t-1} + \boldsymbol{b}_t$ where $\odot$ is the element-wise multiplication. Interestingly, we can see that the GRU and LSTM state recurrences resemble the vector formulation. In this section, we show that GRUs and LSTMs are trainable via parallel scan by simplifying and removing several hidden state dependencies from their various gates. Building on this, we further simplify these RNNs by removing their constraints on output range, (i.e., $\tanh$) and ensuring the outputs are time-independent in scale. Combining the steps, we describe minimal versions of GRUs and LSTMs (minGRUs and minLSTMs) that are trainable via parallel scan and perform comparably to Transformers and recently proposed sequence methods.

3.1 A Minimal GRU: minGRU

3.1.1 Step 1: Drop previous state dependencies from gates

Revisiting GRU's hidden state recurrence which works as follows:

$$\boldsymbol{h}_t = (\mathbf{1} - \boldsymbol{z}_t) \odot \boldsymbol{h}_{t-1} + \boldsymbol{z}_t \odot \tilde{\boldsymbol{h}}_t$$

We can observe that the recurrence resembles the aforementioned parallel scan's formulation where $\boldsymbol{a}_t \leftarrow (\mathbf{1} - \boldsymbol{z}_t)$, $\boldsymbol{b}_t \leftarrow \boldsymbol{z}_t \odot \tilde{\boldsymbol{h}}_t$, and $\boldsymbol{v}_t \leftarrow \boldsymbol{h}_t$. However, $\boldsymbol{z}_t$ and $\tilde{\boldsymbol{h}}_t$ are dependent on previous hidden states $\boldsymbol{h}_{t-1}$, i.e., $\boldsymbol{z}_t = \sigma(\mathrm{Linear}_{d_h}([\boldsymbol{x}_t, \boldsymbol{h}_{t-1}]))$ and $\tilde{\boldsymbol{h}}_t = \tanh(\mathrm{Linear}_{d_h}([\boldsymbol{x}_t, r_t \odot \boldsymbol{h}_{t-1}]))$. As a result, it is not possible to apply the parallel scan as is since the algorithm's inputs $\boldsymbol{a}_1, \ldots, \boldsymbol{a}_n$ and $\boldsymbol{b}_1, \ldots, \boldsymbol{b}_n$ are conditional on already knowing its outputs $\boldsymbol{h}_1, \ldots, \boldsymbol{h}_{n-1}$.

We can remedy this by simplifying GRUs, removing their previous hidden state (i.e., $\boldsymbol{h}_{t-1}$) dependencies. Specifically, the changes are as follows:

$$\begin{aligned}
\boldsymbol{z}_t &= \sigma(\mathrm{Linear}_{d_h}([\boldsymbol{x}_t, \boldsymbol{h}_{t-1}])) \\
\boldsymbol{r}_t &= \sigma(\mathrm{Linear}_{d_h}([\boldsymbol{x}_t, \boldsymbol{h}_{t-1}])) \\
\tilde{\boldsymbol{h}}_t &= \tanh(\mathrm{Linear}_{d_h}([\boldsymbol{x}_t, \boldsymbol{r}_t \odot \boldsymbol{h}_{t-1}]))
\end{aligned}
\quad \Rightarrow \quad
\begin{aligned}
\boldsymbol{z}_t &= \sigma(\mathrm{Linear}_{\boldsymbol{d}_h}(\boldsymbol{x}_t)) \\
\tilde{\boldsymbol{h}}_t &= \tanh(\mathrm{Linear}_{\boldsymbol{d}_h}(\boldsymbol{x}_t))
\end{aligned}$$

By removing the dependence on $\boldsymbol{h}_{t-1}$ from the candidate hidden state $\tilde{\boldsymbol{h}}_t$, the reset gate $\boldsymbol{r}_t$ that would control $\boldsymbol{h}_{t-1}$ weight is also no longer needed and is removed. Without the dependencies on previous hidden states, the inputs to the algorithm $\boldsymbol{a}_1, \ldots, \boldsymbol{a}_n$ and $\boldsymbol{b}_1, \ldots, \boldsymbol{b}_n$ are all easily computed in parallel and can thus be used to compute $\boldsymbol{h}_1, \ldots, \boldsymbol{h}_n$ efficiently via the parallel scan.

Although there are theoretical concerns about the absence of hidden state dependencies (Merrill et al., 2024), there is substantial empirical evidence supporting the effectiveness of models that omit these dependencies, such as xLSTM (Beck et al., 2024) and Mamba (Gu & Dao, 2024). Notably, in the xLSTM paper, their fully parallelized version (xLSTM[1:0]), which eliminates hidden state dependencies, performed similarly to — and in some cases, better than — versions that retain these dependencies (e.g., xLSTM[7:1]). Rather than explicitly modelling dependencies, these models can learn long-range dependencies by stacking multiple layers.

3.1.2 Step 2: Drop range restriction of candidate states

In GRU's hidden state recurrence, the proportion carried over from the previous hidden state $(\mathbf{1} - \boldsymbol{z}_t)$ and the amount added for the new candidate hidden state $(\boldsymbol{z}_t)$ sum to 1. As a result, the scale of GRU's hidden state value is time-independent. Instead, the scale of its hidden state depends on that of its candidate hidden states $\tilde{\boldsymbol{h}}_t$. The hyperbolic tangent function $(\tanh)$ plays a crucial role in LSTMs and GRUs, restricting the range of (candidate) hidden states, i.e., $\tilde{\boldsymbol{h}}_t, \boldsymbol{h}_t \in (-1, 1)^{d_h}$. The $\tanh$ helps stabilize the training and mitigates vanishing gradients that result from applying sigmoid (σ) activations to linear transformations of the hidden state (e.g., $\boldsymbol{z}_t = \sigma(\mathrm{Linear}_{d_h}([\boldsymbol{x}_t, \boldsymbol{h}_{t-1}]))$). In the previous step, these hidden state dependencies were removed. As such, we can simplify GRU further by removing the range restriction $(\tanh)$ on the (candidate) hidden states as follows:

$$\tilde{\boldsymbol{h}}_t = \tanh(\mathrm{Linear}_{d_h}(\boldsymbol{x}_t)) \quad \Rightarrow \quad \tilde{\boldsymbol{h}}_t = \mathrm{Linear}_{d_h}(\boldsymbol{x}_t)$$

3.1.3 minGRU

Combining the two simplification steps results in a minimal version of GRU (minGRU):

GRU

$$\begin{aligned}
\boldsymbol{h}_t &= (\mathbf{1} - \boldsymbol{z}_t) \odot \boldsymbol{h}_{t-1} + \boldsymbol{z}_t \odot \tilde{\boldsymbol{h}}_t \\
\boldsymbol{z}_t &= \sigma(\mathrm{Linear}_{d_h}([\boldsymbol{x}_t, \boldsymbol{h}_{t-1}])) \\
\boldsymbol{r}_t &= \sigma(\mathrm{Linear}_{d_h}([\boldsymbol{x}_t, \boldsymbol{h}_{t-1}])) \\
\tilde{\boldsymbol{h}}_t &= \tanh(\mathrm{Linear}_{d_h}([\boldsymbol{x}_t, \boldsymbol{r}_t \odot \boldsymbol{h}_{t-1}]))
\end{aligned}$$

$$\Rightarrow$$

minGRU

$$\begin{aligned}
\boldsymbol{h}_t &= (\mathbf{1} - \boldsymbol{z}_t) \odot \boldsymbol{h}_{t-1} + \boldsymbol{z}_t \odot \tilde{\boldsymbol{h}}_t \\
\boldsymbol{z}_t &= \sigma(\mathrm{Linear}_{d_h}(\boldsymbol{x}_t)) \\
\tilde{\boldsymbol{h}}_t &= \mathrm{Linear}_{d_h}(\boldsymbol{x}_t)
\end{aligned}$$

The resulting model is significantly more efficient than the original GRU (1) requiring only $O(2d_h d_x)$ parameters instead of GRU's $O(3d_h(d_x + d_h))$ parameters where d_x, d_h corresponds to the sizes of x_t and h_t respectively. In terms of training, minGRU (2) can be trained in parallel using the parallel scan algorithm, speeding up training significantly. In Section 4.1, we show that this corresponded to a $175\times$ speedup in training steps for a sequence length of 512 on a T4 GPU. The parameter efficiency gains are also significant. Typically, in RNNs, state expansion is performed (i.e., $d_h = \alpha d_x$ where $\alpha \geq 1$) allowing the models to more readily learn features from their inputs. minGRU uses approximately $33\%, 22\%, 17\%$, or 13% of parameters compared to GRU when $\alpha = 1, 2, 3$, or 4 respectively.

3.2 A Minimal LSTM: minLSTM

3.2.1 Step 1: Drop previous state dependencies from gates

Revisiting LSTMs, we focus on their cell state recurrence which works as follows:

$$\boldsymbol{c}_t = \boldsymbol{f}_t \odot \boldsymbol{c}_{t-1} + \boldsymbol{i}_t \odot \tilde{\boldsymbol{c}}_t$$

Similar to GRU's hidden state, we can see that LSTM's cell state recurrence resembles the aforementioned parallel scan's formulation $\boldsymbol{v}_t = \boldsymbol{a}_t \odot \boldsymbol{v}_{t-1} + \boldsymbol{b}_t$ where $\boldsymbol{a}_t \leftarrow \boldsymbol{f}_t$, $\boldsymbol{b}_t \leftarrow \boldsymbol{i}_t \odot \tilde{\boldsymbol{c}}_t$, and $\boldsymbol{v}_t \leftarrow \boldsymbol{c}_t$. However, $\boldsymbol{f}_t$, $\boldsymbol{i}_t$ and $\tilde{\boldsymbol{c}}_t$ are dependent on the previous hidden state $\boldsymbol{h}_t$. As such, LSTM's cell state recurrence is unable to apply the parallel scan algorithm as is. We can address this in a similar fashion to GRU by removing their hidden state dependencies as follows:

$$\begin{aligned}
\boldsymbol{f}_t &= \sigma(\mathrm{Linear}_{d_h}([\boldsymbol{x}_t, \boldsymbol{h}_{t-1}])) \\
\boldsymbol{i}_t &= \sigma(\mathrm{Linear}_{d_h}([\boldsymbol{x}_t, \boldsymbol{h}_{t-1}])) \\
\tilde{\boldsymbol{c}}_t &= \tanh(\mathrm{Linear}_{d_h}([\boldsymbol{x}_t, \boldsymbol{h}_{t-1}]))
\end{aligned}
\quad \Rightarrow \quad
\begin{aligned}
\boldsymbol{f}_t &= \sigma(\mathrm{Linear}_{d_h}(\boldsymbol{x}_t)) \\
\boldsymbol{i}_t &= \sigma(\mathrm{Linear}_{d_h}(\boldsymbol{x}_t)) \\
\tilde{\boldsymbol{c}}_t &= \tanh(\mathrm{Linear}_{d_h}(\boldsymbol{x}_t))
\end{aligned}$$

3.2.2 Step 2: Drop range restriction of candidate states

Similar to GRUs, LSTMs leverage the hyperbolic tangent function ($\tanh$) to restrict the range of its states between $(-1, 1)$. LSTMs apply the range restriction twice: once when computing the candidate cell state and once computing its hidden state. In this step, we drop both as follows:

$$\begin{aligned}
\tilde{\boldsymbol{c}}_t &= \tanh(\mathrm{Linear}_{d_h}(\boldsymbol{x}_t)) \\
\boldsymbol{h}_t &= \boldsymbol{o}_t \odot \tanh(\boldsymbol{c}_t)
\end{aligned}
\quad \Rightarrow \quad
\begin{aligned}
\tilde{\boldsymbol{c}}_t &= \mathrm{Linear}_{d_h}(\boldsymbol{x}_t) \\
\boldsymbol{h}_t &= \boldsymbol{o}_t \odot \boldsymbol{c}_t
\end{aligned}$$

3.2.3 Step 3: Ensure output is time-independent in scale

In many sequence modelling settings (e.g., text generation), the optimization objective/target is time-independent in scale. Recall LSTM's cell state recurrence $\boldsymbol{c}_t = \boldsymbol{f}_t \odot \boldsymbol{c}_{t-1} + \boldsymbol{i}_t \odot \tilde{\boldsymbol{c}}_t$ where $\boldsymbol{i}_t, \boldsymbol{f}_t \in (0,1)^{d_h}$, and GRU's hidden state recurrence[2], $\boldsymbol{h}_t^{GRU} = (\mathbf{1} - \boldsymbol{z}_t) \odot \boldsymbol{h}_{t-1}^{GRU} + \boldsymbol{z}_t \odot \tilde{\boldsymbol{h}}_t^{GRU}$ where $\boldsymbol{z}_t \in (0,1)^{d_h}$. GRUs retain $(\mathbf{1} - \boldsymbol{z}_t) \in (0,1)$ of the previous hidden state and add $\boldsymbol{z}_t$ of the new candidate state. Since these proportions sum to $\mathbf{1}$, the model ensures its outputs (i.e., hidden states) are *time-independent* in scale. In contrast, LSTM's forget and input gates are computed independently (e.g., $\boldsymbol{f}_t, \boldsymbol{i}_t \to \mathbf{1}$ or $\boldsymbol{f}_t, \boldsymbol{i}_t \to \mathbf{0}$), making its cell states *time-dependent* in scale[3] and optimization more difficult. As such, we ensure LSTM's output is time-independent in scale.

To do so, we can simply normalize the two gates, i.e., $\boldsymbol{f}'_t, \boldsymbol{i}'_t \leftarrow \frac{\boldsymbol{f}_t}{\boldsymbol{f}_t + \boldsymbol{i}_t}, \frac{\boldsymbol{i}_t}{\boldsymbol{f}_t + \boldsymbol{i}_t}$, ensuring that $\boldsymbol{f}'_t + \boldsymbol{i}'_t = \mathbf{1}$ and the scale of LSTM's cell state is time-independent. Ensuring that the hidden state is time-independent in scale, we also drop the output gate $\boldsymbol{o}_t$ which scales the hidden state. Without the output gate, the normalized hidden state is equal to the cell state, i.e., $\boldsymbol{h}_t = \boldsymbol{o}_t \odot \boldsymbol{c}_t \Rightarrow \boldsymbol{h}_t = \boldsymbol{c}_t$, making having both a hidden and cell state unnecessary. As such, we drop the cell state as well. In summary, the modifications are as follows:

$$\begin{aligned}
\boldsymbol{h}_t &= \boldsymbol{o}_t \odot \boldsymbol{c}_t \\
\boldsymbol{o}_t &= \sigma(\mathrm{Linear}_{d_h}(\boldsymbol{x}_t)) \\
\boldsymbol{c}_t &= \boldsymbol{f}_t \odot \boldsymbol{c}_{t-1} + \boldsymbol{i}_t \odot \tilde{\boldsymbol{c}}_t \\
\tilde{\boldsymbol{c}}_t &= \mathrm{Linear}_{d_h}(\boldsymbol{x}_t)
\end{aligned}
\quad \Rightarrow \quad
\begin{aligned}
\boldsymbol{h}_t &= \boldsymbol{f}'_t \odot \boldsymbol{h}_{t-1} + \boldsymbol{i}'_t \odot \tilde{\boldsymbol{h}}_t \\
\tilde{\boldsymbol{h}}_t &= \mathrm{Linear}_{d_h}(\boldsymbol{x}_t) \\
\boldsymbol{f}'_t, \boldsymbol{i}'_t &\leftarrow \frac{\boldsymbol{f}_t}{\boldsymbol{f}_t + \boldsymbol{i}_t}, \frac{\boldsymbol{i}_t}{\boldsymbol{f}_t + \boldsymbol{i}_t}
\end{aligned}$$

Notably, GRUs do not need this step as their outputs are already time-independent in scale.

3.2.4 minLSTM

Combining the three steps results in a minimal version of LSTM (minLSTM):

[2] A superscript is added to differentiate GRU's hidden state from LSTM's.

[3] For example, $\boldsymbol{c}_t \to \boldsymbol{c}_0 + \sum_{i=1}^{t} \tilde{\boldsymbol{c}}_t$ when $\boldsymbol{f}_{1:t}, \boldsymbol{i}_{1:t} \to 1$, growing in scale as the sequence length increases.

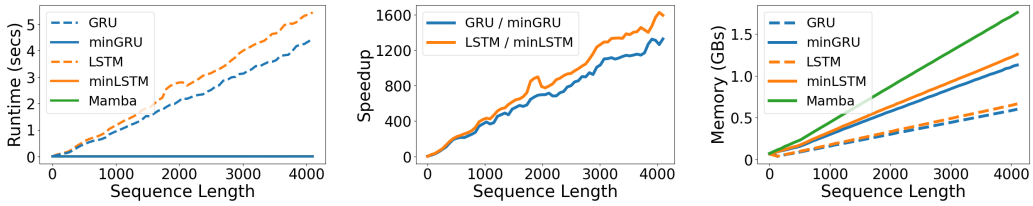

Figure 1: Training runtime (left), speedup (middle), and memory footprint (right) on a T4 GPU for a batch size of 64. In the training runtime plot (left), minGRU, minLSTM, and Mamba lines overlap. These methods are approximately the same in training runtime.

LSTM

$$\begin{aligned}
\boldsymbol{h}_t &= \boldsymbol{o}_t \odot \tanh(\boldsymbol{c}_t) \\
\boldsymbol{o}_t &= \sigma(\text{Linear}_{d_h}([\boldsymbol{x}_t, \boldsymbol{h}_{t-1}])) \\
\boldsymbol{c}_t &= \boldsymbol{f}_t \odot \boldsymbol{c}_{t-1} + \boldsymbol{i}_t \odot \tilde{\boldsymbol{c}}_t \\
\boldsymbol{f}_t &= \sigma(\text{Linear}_{d_h}([\boldsymbol{x}_t, \boldsymbol{h}_{t-1}])) \\
\boldsymbol{i}_t &= \sigma(\text{Linear}_{d_h}([\boldsymbol{x}_t, \boldsymbol{h}_{t-1}])) \\
\tilde{\boldsymbol{c}}_t &= \tanh(\text{Linear}_{d_h}([\boldsymbol{x}_t, \boldsymbol{h}_{t-1}]))
\end{aligned}$$

$$\Rightarrow$$

minLSTM

$$\begin{aligned}
\boldsymbol{h}_t &= \boldsymbol{f}'_t \odot \boldsymbol{h}_{t-1} + \boldsymbol{i}'_t \odot \tilde{\boldsymbol{h}}_t \\
\boldsymbol{f}_t &= \sigma(\text{Linear}_{d_h}(\boldsymbol{x}_t)) \\
\boldsymbol{i}_t &= \sigma(\text{Linear}_{d_h}(\boldsymbol{x}_t)) \\
\tilde{\boldsymbol{h}}_t &= \text{Linear}_{d_h}(\boldsymbol{x}_t) \\
\boldsymbol{f}'_t, \boldsymbol{i}'_t &\leftarrow \frac{\boldsymbol{f}_t}{\boldsymbol{f}_t + \boldsymbol{i}_t}, \frac{\boldsymbol{i}_t}{\boldsymbol{f}_t + \boldsymbol{i}_t}
\end{aligned}$$

The minimal version (minLSTM) is significantly more efficient (1) requiring only $O(3d_h d_x)$ parameters compared to LSTM's $O(4d_h(d_x + d_h))$. Furthermore, minLSTM (2) can be trained in parallel using the parallel scan algorithm, speeding up training significantly. For example, in Section 4.1, we found that minLSTM corresponded to a $235\times$ speedup for a sequence of length 512 compared to LSTM on a T4 GPU. In terms of parameter efficiency, minLSTM uses only $38\%, 25\%, 19\%$, or 15% of parameters compared to LSTM when $\alpha = 1, 2, 3$, or 4 respectively where $d_h = \alpha d_x$.

4 Were RNNs All We Needed?

In this section, we compare the minimal versions (minLSTMs and minGRUs) with their traditional counterparts (LSTMs and GRUs) and modern sequence models. Pseudocode, PyTorch implementation, and detailed information regarding the experiment setup are available in the Appendix.

4.1 Minimal LSTMs and GRUs are very efficient

At test time, recurrent sequence models are typically rolled out sequentially, which makes inference relatively efficient. However, the main bottleneck for traditional RNNs lies in their training, which requires linear time due to backpropagation through time (BPTT). This computational inefficiency contributed to the eventual deprecation of many earlier RNN-based models. Recent advances, however, have sparked renewed interest in recurrent sequence models, driven by new architectures that enable parallelized training (Gu et al., 2021).

In this section, we compare the resource requirements for training traditional RNNs (LSTM and GRU)[4], their simplified counterparts (minLSTM and minGRU), and a recent state-of-the-art sequence model, specifically Mamba (Gu & Dao, 2024), which has gained significant popularity in recent work.

For our experiments, we use a batch size of 64 and vary the sequence length. We measure both the total runtime and memory complexity involved in performing a forward pass, computing the loss,

[4]PyTorch's built-in RNNs have highly optimized low-level GPU implementations. As such, for fairness, in our experiments, we compared GRU, LSTM, minGRU, and minLSTM written in plain Pytorch.

and performing backpropagation to compute gradients. To ensure a fair and direct comparison, all models were tested with the same number of layers.

Runtime. In terms of runtime (see Figure 1 (left)), the simplified versions of LSTM and GRU (minLSTM and minGRU) Mamba achieve similar runtimes. Averaging over 100 runs, the runtime for sequence lengths of 512 for minLSTM, minGRU, and Mamba were 2.97, 2.72, and 2.71 milliseconds respectively. For a sequence with length 4096, the runtime were 3.41, 3.25, and 3.15 respectively. In contrast, the traditional RNN counterparts (LSTMs and GRUs) required a runtime that scaled linearly with respect to sequence length. For a sequence length of 512, minGRUs and minLSTMs were $175\times$ and $235\times$ faster per training step (see Figure 1 (middle)) than GRUs and LSTMs on a T4 GPU. The improvement is even more significant as sequences grow in length with minGRUs and minLSTMs being $1324\times$ and $1361\times$ faster for a sequence length of 4096. As such, in a setting where minGRU would take a day to finish training for a fixed number of epochs, its traditional counterpart GRU could take over 3 years.

Memory. By leveraging a parallel scan algorithm to compute the outputs in parallel efficiently, minGRU, minLSTM, and Mamba create a larger computational graph, thus needing more memory compared to traditional RNNs (see Figure 1 (right)). The minimal variants (minGRU and minLSTM) use $\sim 88\%$ more memory compared to their traditional counterpart. Mamba uses 56% more memory compared to minGRU. In practice, however, runtime is the bottleneck when training RNNs.

Effect of removing $\boldsymbol{h}_{t-1}$. The original LSTM and GRU compute their various gates using their inputs $\boldsymbol{x}_t$ and previous hidden states $\boldsymbol{h}_{t-1}$. These models leverage their time-dependent gates to learn complex functions. However, minLSTM and minGRU's training efficiencies are achieved by dropping their gates' dependencies on the previous hidden states $\boldsymbol{h}_{t-1}$. As a result, minLSTM and minGRU's gates are dependent only on their inputs $\boldsymbol{x}_t$, resulting in a simpler recurrent module. As such, the gates of a model consisting of a single layer of minLSTM or minGRU are *time-independent* due to being conditioned on *time-independent* inputs $\boldsymbol{x}^{(1)}_{1:n}$.

However, in deep learning, models are constructed by stacking modules. Although the inputs to the first layer $\boldsymbol{x}^{(1)}_{1:n}$ is *time-independent*, its outputs $\boldsymbol{h}^{(1)}_{1:n}$ are *time-dependent* and are used as the inputs to the second layer, i.e., $\boldsymbol{x}^{(2)}_{1:n} \leftarrow \boldsymbol{h}^{(1)}_{1:n}$. As such, beginning from the second layer onwards, minLSTM and minGRU's gates will also be time-dependent, resulting in the modelling of more complex functions. In Table 1, we compare the performance of the models with varying numbers of layers on the Selective Copying Task from the Mamba paper (Gu & Dao, 2024). We can immediately see the impact of the time dependencies: increasing the number of layers to 2 or more drastically increases the model's performance.

Model	# Layers	Accuracy
MinLSTM	1	37.6 ± 2.0
	2	85.7 ± 5.8
	3	96.0 ± 2.8
MinGRU	1	37.0 ± 2.3
	2	96.8 ± 3.2
	3	99.5 ± 0.2

Table 1: Comparison of the number of layers on the Selective Copying Task (Gu & Dao, 2024).

Training Stability. Another effect of the number of layers is increased stability with decreased variance in the accuracy as the number of layers increases (see Table 1). Furthermore, although minLSTM and minGRU both solve the Selective Copying task, we can see that minGRU is an empirically more stable method than minLSTM, solving the task with more consistency and lower variance. minLSTM discards old information and adds new information, controlling the ratio with two sets of parameters (forget and input gate). During training, the two sets of parameters are tuned in different directions, making the ratio harder to control and optimize. In contrast, minGRU's discarding and adding of information is controlled by a single set of parameters (update gate), making it easier to optimize.

4.2 Minimal RNNs perform surprisingly well

In the previous section, we highlighted the substantial efficiency gains achieved by simplifying traditional RNNs. In this section, we focus on the empirical performance of these minimal versions of LSTMs and GRUs, comparing them to several well-known sequence models. It is important to note that the primary goal of our work is not to attain the best performance on specific tasks but to

Dataset	DT	DS4	DAaren	DMamba	minLSTM	minGRU
HalfCheetah-M	42.6	42.5	42.2	42.8	42.7 ± 0.7	43.0 ± 0.4
Hopper-M	68.4	54.2	80.9	83.5	85.0 ± 4.4	79.4 ± 8.2
Walker-M	75.5	78.0	74.4	78.2	72.0 ± 7.5	73.3 ± 3.3
HalfCheetah-M-R	37.0	15.2	37.9	39.6	38.6 ± 1.1	38.5 ± 1.1
Hopper-M-R	85.6	49.6	77.9	82.6	88.5 ± 4.7	90.5 ± 0.9
Walker-M-R	71.2	69.0	71.4	70.9	69.7 ± 10.7	72.8 ± 8.9
HalfCheetah-M-E	88.8	92.7	75.7	91.9	85.4 ± 1.7	86.3 ± 0.5
Hopper-M-E	109.6	110.8	103.9	111.1	110.3 ± 1.6	109.7 ± 2.7
Walker-M-E	109.3	105.7	110.5	108.3	110.3 ± 0.5	110.3 ± 0.4
Average	76.4	68.6	75.0	78.8	78.1	78.2

Table 3: Reinforcement Learning results on the D4RL (Fu et al., 2020) datasets. We report the expert normalized returns (higher is better), following (Fu et al., 2020), averaged across five random seeds. The minimal versions of LSTM and GRU, minLSTM and minGRU outperform Decision S4 (David et al., 2023) and perform comparably with Decision Mamba (Ota, 2024), (Decision) Aaren (Feng et al., 2024) and Decision Transformer (Chen et al., 2021).

demonstrate that simplifying traditional RNN architectures can yield competitive results, comparable to those of modern, state-of-the-art sequence models.

Selective Copy. We begin by considering the Selective Copying task, originally introduced in the influential Mamba paper (Gu & Dao, 2024). This task served as a key benchmark that demonstrated the improvements made by Mamba's state-space model, S6, over previous state-of-the-art models such as S4 (Gu et al., 2021) and Hyena (Poli et al., 2023). The task requires models to perform content-aware reasoning, where they must selectively memorize relevant tokens while filtering out irrelevant ones.

Model	Layer	Accuracy
H3	Hyena	30.1
Mamba	Hyena	28.4
S4	S4	18.3
H3	S4	57.0
Mamba	S4	56.4
S4	S6	97.0
H3	S6	99.7
Mamba	S6	99.8
minGRU	minGRU	99.5 ± 0.2
minLSTM	minLSTM	96.0 ± 2.8

Table 2: Selective Copy Task. minLSTM, minGRU, and Mamba's S6 (Gu & Dao, 2024) are capable of solving this task. Other methods such as S4, H3, and Hyena at best only partially solve the task.

In Table 2, we compare the simplified versions of LSTMs and GRUs (minLSTM and minGRU) with several well-known recurrent sequence models that can be trained in parallel, including S4 (Gu et al., 2021), H3 (Fu et al., 2023), Hyena (Poli et al., 2023), and Mamba (S6) (Gu & Dao, 2024). The results for these baselines are directly quoted from the Mamba paper. Among these, only Mamba's S6 model succeeds in solving the task.

Both minGRU and minLSTM are able to solve the Selective Copying task as well, achieving performance comparable to S6 and surpassing all other baseline models. The success of these minimal versions highlights the effectiveness of LSTMs and GRUs, which utilize content-aware gating mechanisms. This enables the simplified architectures to solve the task—something that many other modern sequence models fail to achieve.

Reinforcement Learning. Next, we consider the MuJoCo locomotion tasks from the D4RL benchmark (Fu et al., 2020). Specifically, we consider the three environments: HalfCheetah, Hopper, and Walker. For each environment, the models are trained on three datasets of varying data quality: Medium (M), Medium-Replay (M-R), and Medium-Expert (M-E).

In Table 3, we compare minLSTM and minGRU with various Decision Transformer variants, including the original Decision Transformer (DT) (Chen et al., 2021), Decision S4 (DS4) (David et al., 2023), Decision Mamba (Ota, 2024), and (Decision) Aaren (Feng et al., 2024). The baseline results are retrieved from the Decision Mamba and Aaren papers. minLSTM and minGRU outperform Decision S4 and achieve performance competitive with Decision Transformer, Aaren,

and Mamba. Unlike other recurrent methods, Decision S4 is a model whose recurrence transitions are not input-aware, affecting their performance. In terms of average score across the $3 \times 3 = 9$ datasets, minLSTM and minGRU outperform all the baselines except for Decision Mamba where the difference is marginal.

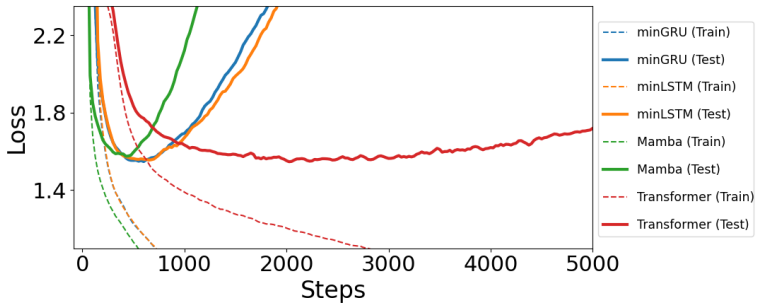

Figure 2: Language Modelling results on the Shakespeare dataset. Minimal versions of decade-old RNNs (LSTMs and GRUs) performed comparably to Mamba and Transformers. Transformers required $\sim 2.5\times$ more training steps to achieve comparable performance, overfitting eventually.

Language Modelling. Finally, we consider a language modelling task. In this setting, we train a character-level GPT on the works of Shakespeare using the nanoGPT (Karpathy, 2022) framework. In Figure 2, we plot the learning curves with a cross-entropy loss comparing the proposed minimal LSTM and GRU (minLSTM and minGRU) with Mamba and Transformers. We found that minGRU, minLSTM, Mamba, and Transformers achieved comparable test losses of 1.548, 1.555, 1.575, and 1.547 respectively. Mamba performed slightly worse than the other models but trained faster, particularly in the early stages, achieving its best performance at 400 steps while minGRU and minLSTM continued training until 575 and 625 steps respectively. In contrast, Transformers trained significantly slower, requiring 2000 steps ($\sim 2.5\times$) more training steps than minGRU to achieve comparable performance, making it significantly slower and more resource-intensive to train (quadratic complexity compared to minGRU, minLSTM, and Mamba's linear complexity).

5 Related Work

In this section, we briefly discuss the similarities and differences between recently proposed efficient recurrent sequence models and our simplified versions of traditional RNNs, minLSTM and minGRU. An extended version of this section is included in the Appendix. For a more comprehensive overview of the resurgence of efficient recurrent sequence models, we refer the reader to recent survey works (Tiezzi et al., 2024a;b). Roughly speaking, recent recurrent sequence models have been developed in three directions:

(Deep) State-Space Models (SSMs). Building on continuous-time linear systems, Gu et al. (2021) introduced S4, a state-space model that can be unrolled like an RNN during inference and trained similarly to a convolutional neural network. S4's success paved the way for numerous subsequent developments in the field (Gu et al., 2022; Gupta et al., 2022; Hasani et al., 2023; Smith et al., 2023) and their applications across various domains such as language processing (Mehta et al., 2023) and audio analysis (Goel et al., 2022). More recently, Mamba emerged as a significant breakthrough in SSMs, surpassing previous models and attracting considerable attention. One of the key innovations in Mamba was the introduction of S6, a state-space model with input-dependent transition matrices, contrasting with earlier models that used input-independent transition matrices. The success of Mamba and other state-space models has led to the publication of several comprehensive surveys on the topic (Wang et al., 2024; Patro & Agneeswaran, 2024; Qu et al., 2024).

Recurrent Versions of Attention. Another popular direction is that of attention, specifically related to linear attention (Katharopoulos et al., 2020). For example, Sun et al. (2023) and Qin et al. (2023) introduced linear attention models that use an input-independent gating mechanism (decay factor). In contrast, Katsch (2023) and Yang et al. (2024) proposed linear attention variants that use input-dependent gating. Recently, Feng et al. (2024) showed that softmax attention can also be viewed as an RNN and proposed a recurrent model based on their RNN formulation.

Parallelizable RNNs. Lastly, several papers have approached the problem by revisiting and parallelizing RNNs. Bradbury et al. (2017) modified classical gated RNNs to leverage convolutional layers for efficiency, applying them temporally. Martin & Cundy (2018) showed that RNNs with linear dependencies can be efficiently trained via a parallel scan. Building on this, the authors propose to augment LSTMs with a linear surrogate model allowing the LSTM to be trained via a parallel scan. More recently, Orvieto et al. (2023) proposed a linear gated RNN that leverages complex diagonal recurrences and an exponential parameterization, achieving comparable performance to state-space models. Qin et al. (2024b) introduced HGRN whose token mixer HGRU is a linear gated RNN augmented with complex value (polar coordinate) recurrences, lower bounds on their forget gate, and an output gate. HGRN2 (Qin et al., 2024a) improved HGRN by incorporating state expansion. Beck et al. (2024) proposed extends LSTM using exponential gating and a normalizer state, proposes xLSTM consisting of parallelizable (mLSTM) and sequential-only (sLSTM) versions. Notably, mLSTM removes the hidden state dependencies to enable parallelization, introduces a matrix memory cell, and uses a query vector for retrieval from the memory. This makes mLSTM more efficient and parallelizable but still retains considerable complexity.

6 Conclusion

A common trend in these sequence modelling developments — including state-space models like Mamba and new RNN variants like xLSTM — is the increasing architectural and algorithmic complexity designed to achieve parallelizability and competitive performance. In this work, we challenge this prevailing trend. By revisiting well-established RNNs (LSTMs and GRUs), we demonstrate that removing the previous state dependencies from their gates enables efficient parallel training using the parallel scan algorithm. Further simplifying these models, we eliminate constraints on their output range, resulting in minimal versions (minLSTM and minGRU). Our empirical results show that these simplified RNNs can achieve competitive performance and computational efficiency across a range of benchmarks compared to modern recurrent sequence models, challenging the prevailing push towards greater complexity. Based on our findings, we ask: "Were RNNs all we needed?"

Limitations

Modern models such as Mamba and xLSTM were run on modern A100 GPUs with 80 GB of memory. In contrast, our experiments were conducted on older GPUs (i.e., P100, T4, and Quadro 5000) with only 16 GB of memory (roughly 20% of the memory available to the other models). These hardware constraints significantly impacted our ability to perform large-scale experiments, especially on large datasets. To accommodate the memory limitations, we used gradient accumulation for training some tasks, reducing the effective batch size by half, which resulted in significantly slower training times. While this approach allowed us to run experiments within the available memory constraints, it also limited the scale of our evaluations.

Despite these limitations, we believe that the conclusions drawn from our experiments are likely to generalize to larger-scale settings. The minimal RNNs share fundamental similarities with many state-of-the-art sequence models, which suggests that their performance would likely be consistent with larger datasets given sufficient computational resources.

References

Maximilian Beck, Korbinian Pöppel, Markus Spanring, Andreas Auer, Oleksandra Prudnikova, Michael Kopp, Günter Klambauer, Johannes Brandstetter, and Sepp Hochreiter. xlstm: Extended long short-term memory. *arXiv preprint arXiv:2405.04517*, 2024.

Guy E Blelloch. Prefix sums and their applications. *Technical Report CMU-CS-90-190, School of Computer Science, Carnegie Mellon University*, 1990.

James Bradbury, Stephen Merity, Caiming Xiong, and Richard Socher. Quasi-recurrent neural networks. In *International Conference on Learning Representations*, 2017.

Tom B. Brown, Benjamin Mann, Nick Ryder, Melanie Subbiah, Jared Kaplan, Prafulla Dhariwal, Arvind Neelakantan, Pranav Shyam, Girish Sastry, Amanda Askell, Sandhini Agarwal, Ariel Herbert-Voss, Gretchen Krueger, Tom Henighan, Rewon Child, Aditya Ramesh, Daniel M. Ziegler, Jeff Wu, Clemens Winter, Christopher Hesse, Mark Chen, Eric Sigler, Mateusz Litwin, Scott Gray, Benjamin Chess, Jack Clark, Christopher Berner, Sam McCandlish, Alec Radford, Ilya Sutskever, and Dario Amodei. Language models are few-shot learners. *ArXiv*, abs/2005.14165, 2020.

Lili Chen, Kevin Lu, Aravind Rajeswaran, Kimin Lee, Aditya Grover, Misha Laskin, Pieter Abbeel, Aravind Srinivas, and Igor Mordatch. Decision transformer: Reinforcement learning via sequence modeling. *Advances in neural information processing systems*, 34:15084–15097, 2021.

Kyunghyun Cho, Bart Van Merrienboer, Caglar Gulcehre, Fethi Bougares, Holger Schwenk, and Yoshua Bengio. Learning phrase representations using rnn encoder-decoder for statistical machine translation. In *EMNLP*, 2014.

Shmuel Bar David, Itamar Zimerman, Eliya Nachmani, and Lior Wolf. Decision s4: Efficient sequence-based rl via state spaces layers. In *The Eleventh International Conference on Learning Representations*, 2023.

Gregoire Deletang, Anian Ruoss, Jordi Grau-Moya, Tim Genewein, Li Kevin Wenliang, Elliot Catt, Chris Cundy, Marcus Hutter, Shane Legg, Joel Veness, et al. Neural networks and the chomsky hierarchy. In *The Eleventh International Conference on Learning Representations*, 2023.

Jacob Devlin, Ming-Wei Chang, Kenton Lee, and Kristina Toutanova. Bert: Pre-training of deep bidirectional transformers for language understanding. In *North American Chapter of the Association for Computational Linguistics*, 2019.

Jeffrey L. Elman. Finding structure in time. *Cognitive Science*, 14(2):179–211, 1990. ISSN 0364-0213.

Leo Feng, Frederick Tung, Hossein Hajimirsadeghi, Mohamed Osama Ahmed, Yoshua Bengio, and Greg Mori. Attention as an rnn. *arXiv preprint arXiv:2405.13956*, 2024.

Daniel Y Fu, Tri Dao, Khaled Kamal Saab, Armin W Thomas, Atri Rudra, and Christopher Re. Hungry hungry hippos: Towards language modeling with state space models. In *The Eleventh International Conference on Learning Representations*, 2023.

Justin Fu, Aviral Kumar, Ofir Nachum, George Tucker, and Sergey Levine. D4rl: Datasets for deep data-driven reinforcement learning. *arXiv preprint arXiv:2004.07219*, 2020.

Karan Goel, Albert Gu, Chris Donahue, and Christopher Ré. It's raw! audio generation with state-space models. In *International Conference on Machine Learning*, pp. 7616–7633. PMLR, 2022.

Albert Gu and Tri Dao. Mamba: Linear-time sequence modeling with selective state spaces. *arXiv preprint arXiv:2312.00752*, 2024.

Albert Gu, Tri Dao, Stefano Ermon, Atri Rudra, and Christopher Ré. Hippo: Recurrent memory with optimal polynomial projections. *Advances in neural information processing systems*, 33: 1474–1487, 2020.

Albert Gu, Karan Goel, and Christopher Re. Efficiently modeling long sequences with structured state spaces. In *International Conference on Learning Representations*, 2021.

Albert Gu, Karan Goel, Ankit Gupta, and Christopher Ré. On the parameterization and initialization of diagonal state space models. *Advances in Neural Information Processing Systems*, 35:35971–35983, 2022.

Ankit Gupta, Albert Gu, and Jonathan Berant. Diagonal state spaces are as effective as structured state spaces. *Advances in Neural Information Processing Systems*, 35:22982–22994, 2022.

Ramin Hasani, Mathias Lechner, Tsun-Hsuan Wang, Makram Chahine, Alexander Amini, and Daniela Rus. Liquid structural state-space models. In *The Eleventh International Conference on Learning Representations*, 2023.

Franz A Heinsen. Parallelization of an ubiquitous sequential computation. *arXiv preprint arXiv:2311.06281*, 2023.

S Hochreiter and J Schmidhuber. Long short-term memory. *Neural Computation*, 9(8):1735–1780, 1997.

Andrej Karpathy. NanoGPT. `https://github.com/karpathy/nanoGPT`, 2022.

Angelos Katharopoulos, Apoorv Vyas, Nikolaos Pappas, and François Fleuret. Transformers are rnns: Fast autoregressive transformers with linear attention. In *International conference on machine learning*, pp. 5156–5165. PMLR, 2020.

Tobias Katsch. Gateloop: Fully data-controlled linear recurrence for sequence modeling. *arXiv preprint arXiv:2311.01927*, 2023.

A Krizhevsky. Learning multiple layers of features from tiny images. *Master's thesis, University of Tront*, 2009.

Eric Martin and Chris Cundy. Parallelizing linear recurrent neural nets over sequence length. In *International Conference on Learning Representations*, 2018.

Harsh Mehta, Ankit Gupta, Ashok Cutkosky, and Behnam Neyshabur. Long range language modeling via gated state spaces. In *The Eleventh International Conference on Learning Representations*, 2023.

William Merrill, Jackson Petty, and Ashish Sabharwal. The illusion of state in state-space models. In *Forty-first International Conference on Machine Learning*, 2024.

Nikita Nangia and Samuel Bowman. ListOps: A diagnostic dataset for latent tree learning. In Silvio Ricardo Cordeiro, Shereen Oraby, Umashanthi Pavalanathan, and Kyeongmin Rim (eds.), *Proceedings of the 2018 Conference of the North American Chapter of the Association for Computational Linguistics: Student Research Workshop*, pp. 92–99, New Orleans, Louisiana, USA, June 2018. Association for Computational Linguistics. doi: 10.18653/v1/N18-4013. URL `https://aclanthology.org/N18-4013`.

Antonio Orvieto, Samuel L Smith, Albert Gu, Anushan Fernando, Caglar Gulcehre, Razvan Pascanu, and Soham De. Resurrecting recurrent neural networks for long sequences. In *International Conference on Machine Learning*, pp. 26670–26698. PMLR, 2023.

Toshihiro Ota. Decision mamba: Reinforcement learning via sequence modeling with selective state spaces. *arXiv preprint arXiv:2403.19925*, 2024.

Badri Narayana Patro and Vijay Srinivas Agneeswaran. Mamba-360: Survey of state space models as transformer alternative for long sequence modelling: Methods, applications, and challenges. *arXiv preprint arXiv:2404.16112*, 2024.

Bo Peng, Eric Alcaide, Quentin Anthony, Alon Albalak, Samuel Arcadinho, Stella Biderman, Huanqi Cao, Xin Cheng, Michael Chung, Matteo Grella, et al. Rwkv: Reinventing rnns for the transformer era. *arXiv preprint arXiv:2305.13048*, 2023.

Michael Poli, Stefano Massaroli, Eric Nguyen, Daniel Y Fu, Tri Dao, Stephen Baccus, Yoshua Bengio, Stefano Ermon, and Christopher Ré. Hyena hierarchy: Towards larger convolutional language models. In *International Conference on Machine Learning*, pp. 28043–28078. PMLR, 2023.

Zhen Qin, Dong Li, Weigao Sun, Weixuan Sun, Xuyang Shen, Xiaodong Han, Yunshen Wei, Baohong Lv, Fei Yuan, Xiao Luo, et al. Scaling transnormer to 175 billion parameters. *arXiv preprint arXiv:2307.14995*, 2023.

Zhen Qin, Songlin Yang, Weixuan Sun, Xuyang Shen, Dong Li, Weigao Sun, and Yiran Zhong. Hgrn2: Gated linear rnns with state expansion. *Conference on Language Modeling*, 2024a.

Zhen Qin, Songlin Yang, and Yiran Zhong. Hierarchically gated recurrent neural network for sequence modeling. *Advances in Neural Information Processing Systems*, 36, 2024b.

Haohao Qu, Liangbo Ning, Rui An, Wenqi Fan, Tyler Derr, Xin Xu, and Qing Li. A survey of mamba. *arXiv preprint arXiv:2408.01129*, 2024.

Dragomir R. Radev, Pradeep Muthukrishnan, and Vahed Qazvinian. The ACL Anthology network corpus. In Min-Yen Kan and Simone Teufel (eds.), *Proceedings of the 2009 Workshop on Text and Citation Analysis for Scholarly Digital Libraries (NLPIR4DL)*, pp. 54–61, Suntec City, Singapore, August 2009. Association for Computational Linguistics. URL https://aclanthology.org/W09-3607.

Jimmy TH Smith, Andrew Warrington, and Scott Linderman. Simplified state space layers for sequence modeling. In *The Eleventh International Conference on Learning Representations*, 2023.

Yutao Sun, Li Dong, Shaohan Huang, Shuming Ma, Yuqing Xia, Jilong Xue, Jianyong Wang, and Furu Wei. Retentive network: A successor to transformer for large language models. *arXiv preprint arXiv:2307.08621*, 2023.

Yi Tay, Mostafa Dehghani, Samira Abnar, Yikang Shen, Dara Bahri, Philip Pham, Jinfeng Rao, Liu Yang, Sebastian Ruder, and Donald Metzler. Long range arena: A benchmark for efficient transformers. In *International Conference on Learning Representations*, 2021.

Matteo Tiezzi, Michele Casoni, Alessandro Betti, Marco Gori, and Stefano Melacci. State-space modeling in long sequence processing: A survey on recurrence in the transformer era. *arXiv preprint arXiv:2406.09062*, 2024a.

Matteo Tiezzi, Michele Casoni, Alessandro Betti, Tommaso Guidi, Marco Gori, and Stefano Melacci. On the resurgence of recurrent models for long sequences: Survey and research opportunities in the transformer era. *arXiv preprint arXiv:2402.08132*, 2024b.

Ashish Vaswani, Noam Shazeer, Niki Parmar, Jakob Uszkoreit, Llion Jones, Aidan N Gomez, Łukasz Kaiser, and Illia Polosukhin. Attention is all you need. *Advances in neural information processing systems*, 30(2017), 2017.

Xiao Wang, Shiao Wang, Yuhe Ding, Yuehang Li, Wentao Wu, Yao Rong, Weizhe Kong, Ju Huang, Shihao Li, Haoxiang Yang, et al. State space model for new-generation network alternative to transformers: A survey. *arXiv preprint arXiv:2404.09516*, 2024.

Songlin Yang, Bailin Wang, Yikang Shen, Rameswar Panda, and Yoon Kim. Gated linear attention transformers with hardware-efficient training. In *International Conference on Machine Learning*, 2024.

A Implementation Details: Vanilla Version

In this section, we provide the pseudocode and equivalent PyTorch code for minGRU and minLSTM. When performing repeated multiplications such as in many recurrent sequence models, numerical instabilities are common, especially during training. As such, we trained using a log-space implementation (see Section B) for improved numerical stability.

A.1 Pseudocode: Vanilla Version

A.1.1 minGRU: A Minimal GRU

Algorithm 1 Sequential Mode: Minimal Version of GRU (minGRU)

Input: $\boldsymbol{x}_t, \boldsymbol{h}_{t-1}$
Output: $\boldsymbol{h}_t$
$\boldsymbol{z}_t \leftarrow \sigma(\text{Linear}_{d_h}(\boldsymbol{x}_t))$
$\tilde{\boldsymbol{h}}_t \leftarrow \text{Linear}_{d_h}(\boldsymbol{x}_t)$
$\boldsymbol{h}_t \leftarrow (\mathbf{1} - \boldsymbol{z}_t) \odot \boldsymbol{h}_{t-1} + \boldsymbol{z}_t \odot \tilde{\boldsymbol{h}}_t$

Algorithm 2 Parallel Mode: Minimal Version of GRU (minGRU)

Input: $\boldsymbol{x}_{1:t}, \boldsymbol{h}_0$
Output: $\boldsymbol{h}_{1:t}$
$\boldsymbol{z}_{1:t} \leftarrow \sigma(\text{Linear}_{d_h}(\boldsymbol{x}_{1:t}))$
$\tilde{\boldsymbol{h}}_{1:t} \leftarrow \text{Linear}_{d_h}(\boldsymbol{x}_{1:t})$
$\boldsymbol{h}_{1:t} \leftarrow \text{ParallelScan}((\mathbf{1} - \boldsymbol{z}_{1:t}), [\boldsymbol{h}_0, \boldsymbol{z}_{1:t} \odot \tilde{\boldsymbol{h}}_{1:t}])$

A.1.2 minLSTM: A Minimal LSTM

Algorithm 3 Sequential Mode: Minimal Version of LSTM (minLSTM)

Input: $\boldsymbol{x}_t, \boldsymbol{h}_{t-1}$
Output: $\boldsymbol{h}_t$
$\boldsymbol{f}_t \leftarrow \sigma(\text{Linear}_{d_h}(\boldsymbol{x}_t))$
$\boldsymbol{i}_t \leftarrow \sigma(\text{Linear}_{d_h}(\boldsymbol{x}_t))$
$\boldsymbol{f}'_t, \boldsymbol{i}'_t \leftarrow \frac{\boldsymbol{f}_t}{\boldsymbol{f}_t + \boldsymbol{i}_t}, \frac{\boldsymbol{i}_t}{\boldsymbol{f}_t + \boldsymbol{i}_t}$
$\tilde{\boldsymbol{h}}_t \leftarrow \text{Linear}_{d_h}(\boldsymbol{x}_t)$
$\boldsymbol{h}_t \leftarrow \boldsymbol{f}'_t \odot \boldsymbol{h}_{t-1} + \boldsymbol{i}'_t \odot \tilde{\boldsymbol{h}}_t$

Algorithm 4 Parallel Mode: Minimal Version of LSTM (minLSTM)

Input: $\boldsymbol{x}_{1:t}, \boldsymbol{h}_0$
Output: $\boldsymbol{h}_{1:t}$
$\boldsymbol{f}_{1:t} \leftarrow \sigma(\text{Linear}_{d_h}(\boldsymbol{x}_{1:t}))$
$\boldsymbol{i}_{1:t} \leftarrow \sigma(\text{Linear}_{d_h}(\boldsymbol{x}_{1:t}))$
$\boldsymbol{f}'_{1:t}, \boldsymbol{i}'_{1:t} \leftarrow \frac{\boldsymbol{f}_{1:t}}{\boldsymbol{f}_{1:t} + \boldsymbol{i}_{1:t}}, \frac{\boldsymbol{i}_{1:t}}{\boldsymbol{f}_{1:t} + \boldsymbol{i}_{1:t}}$
$\tilde{\boldsymbol{h}}_{1:t} \leftarrow \text{Linear}_{d_h}(\boldsymbol{x}_{1:t})$
$\boldsymbol{h}_{1:t} \leftarrow \text{ParallelScan}(\boldsymbol{f}'_{1:t}, [\boldsymbol{h}_0, \boldsymbol{i}'_{1:t} \odot \tilde{\boldsymbol{h}}_{1:t}])$

A.2 PyTorch Code: Vanilla Version

A.2.1 minGRU: A Minimal GRU

```
    def forward(self, x_t, h_prev):
        # x_t: (batch_size, 1, input_size)
        # h_prev: (batch_size, 1, hidden_size)

        z_t = torch.sigmoid(self.linear_z(x_t))
        h_tilde = self.linear_h(x_t)
        h_t = (1 - z_t) * h_prev + z_t * h_tilde
        return h_t
```

Listing 1: Sequential Mode: Minimal Version of GRU (minGRU)

```
    def forward(self, x, h_0):
        # x: (batch_size, seq_len, input_size)
        # h_0: (batch_size, 1, hidden_size)

        z = torch.sigmoid(self.linear_z(x))
        h_tilde = self.linear_h(x)
        h = parallel_scan((1 - z),
            torch.cat([h_0, z * tilde_h], dim=1))
        return h
```

Listing 2: Parallel Mode: Minimal Version of GRU (minGRU)

A.2.2 minLSTM: A Minimal LSTM

```
    def forward(self, x_t, h_prev):
        # x_t: (batch_size, 1, input_size)
        # h_prev: (batch_size, 1, hidden_size)

        f_t = torch.sigmoid(self.linear_f(x_t))
        i_t = torch.sigmoid(self.linear_i(x_t))
        tilde_h_t = self.linear_h(x_t)
        f_prime_t = f_t / (f_t + i_t)
        i_prime_t = i_t / (f_t + i_t)
        h_t = f_prime_t * h_prev + i_prime_t * tilde_h_t
        return h_t
```

Listing 3: Sequential Mode: Minimal Version of LSTM (minLSTM)

```
    def forward(self, x, h_0):
        # x: (batch_size, seq_len, input_size)
        # h_0: (batch_size, 1, hidden_size)

        f = torch.sigmoid(self.linear_f(x))
        i = torch.sigmoid(self.linear_i(x))
        tilde_h = self.linear_h(x)
        f_prime = f / (f + i)
        i_prime = i / (f + i)
        h = parallel_scan(f_prime,
            torch.cat([h_0, i_prime * tilde_h], dim=1))
        return h
```

Listing 4: Parallel Mode: Minimal Version of LSTM (minLSTM)

B Implementation Details: Log-Space Version (Additional Numerical Stability)

In this section, we detail the log-space version of minLSTM and minGRU for improved numerical stability. During training, the parallel modes are used to avoid backpropagation through time (BPTT), speeding up the training time significantly. At inference time, the sequential modes are used.

B.1 Parallel Scan: Log-Space Implementation

Recall that, the parallel scan's objective is to compute $\boldsymbol{h}_{1:t}$ where $\boldsymbol{h}_k = \boldsymbol{a}_k \odot \boldsymbol{h}_{k-1} + \boldsymbol{b}_k$. In code, the vanilla parallel scan function would take as input: coefficients $\boldsymbol{a}_{1:t}$ and values $\boldsymbol{b}_{0:t}$. The function then outputs $\boldsymbol{h}_{1:t}$. For numerical stability, we consider a log-space implementation which takes as input $\log(\boldsymbol{a}_{1:t})$ and $\log(\boldsymbol{b}_{0:t})$ instead and outputs $\boldsymbol{h}_{1:t}$. The code for the parallel scan in log-space is included below and is based on the code by Heinsen (2023).

```python
def parallel_scan_log(log_coeffs, log_values):
    # log_coeffs: (batch_size, seq_len, input_size)
    # log_values: (batch_size, seq_len + 1, input_size)
    a_star = F.pad(torch.cumsum(log_coeffs, dim=1), (0, 0, 1, 0))
    log_h0_plus_b_star = torch.logcumsumexp(
                                log_values - a_star, dim=1)
    log_h = a_star + log_h0_plus_b_star
    return torch.exp(log_h)[:, 1:]
```

Listing 5: Parallel scan based on Heinsen (2023). This function computes $\boldsymbol{h}_{1:t}$ given log coefficients $\log(\boldsymbol{a}_{1:t})$ and log values $\log(\boldsymbol{b}_{0:t})$.

B.2 Pseudocode: Log-Space Version

For maximal numerical stability, we rewrite the log-space versions of minGRU and minLSTM.

B.2.1 minGRU: A Minimal GRU

Recall minGRU's recurrence is as follows $\boldsymbol{h}_t \leftarrow (\mathbf{1} - \boldsymbol{z}_t) \odot \boldsymbol{h}_{t-1} + \boldsymbol{z}_t \odot \tilde{\boldsymbol{h}}_t$. As such, $\boldsymbol{a}_t \leftarrow (\mathbf{1} - \boldsymbol{z}_t)$ and $\boldsymbol{b}_t \leftarrow \boldsymbol{z}_t \odot \tilde{\boldsymbol{h}}_t$ where $\boldsymbol{z}_t = \sigma(\boldsymbol{k}_t)$ and $\boldsymbol{k}_t = \text{Linear}_{d_h}(x_t)$. As a result, $\log(\boldsymbol{a}_t) \leftarrow \log(\mathbf{1} - \boldsymbol{z}_t)$ and $\log(\boldsymbol{b}_t) \leftarrow \log(\boldsymbol{z}_t) + \log(\tilde{\boldsymbol{h}})_t$. We can break down these down as follows:

$$
\begin{aligned}
\log(\boldsymbol{z}_t) &= \log(\sigma(\boldsymbol{k}_t)) \\
&= \log\left(\frac{1}{1 + \exp(-\boldsymbol{k}_t)}\right) \\
&= -\text{Softplus}(-\boldsymbol{k}_t) \\
\log(\mathbf{1} - \boldsymbol{z}_t) &= \log\left(\frac{\exp(-\boldsymbol{k}_t)}{1 + \exp(-\boldsymbol{k}_t)}\right) \\
&= \log\left(\frac{1}{1 + \exp(\boldsymbol{k}_t)}\right) \\
&= -\text{Softplus}(\boldsymbol{k}_t)
\end{aligned}
$$

where $\boldsymbol{k}_t = \text{Linear}_{d_h}(x_t)$. However, we need to compute $\log(\tilde{\boldsymbol{h}})_t$ which is inconvenient if $\tilde{\boldsymbol{h}}_t$ has some negative values. We could use complex numbers and a complex number version of the parallel scan, but this would result in the parallel scan increasing in complexity. Instead, we propose to ensure that $\tilde{\boldsymbol{h}}_t > 0$. This be can done in a variety of ways. In our experiments, we added a continuous activation function g replacing $\tilde{\boldsymbol{h}}_t \leftarrow \text{Linear}_{d_h}(x_t)$ with $\tilde{\boldsymbol{h}}_t \leftarrow g(\text{Linear}_{d_h}(x_t))$ where $g(x) = \begin{cases} x + 0.5, & \text{if } x \geq 0 \\ \sigma(x), & \text{otherwise} \end{cases}$ and its log: $\log(g(x)) = \begin{cases} \log(x + 0.5), & \text{if } x \geq 0 \\ -\text{Softplus}(-x), & \text{otherwise} \end{cases}$.

At inference time, the sequential mode (Algorithm 5) is used. During training, the parallel mode (Algorithm 6) is used.

Algorithm 5 Sequential Mode: Minimal Version of GRU (minGRU) trained in log-space

Input: $\boldsymbol{x}_t, \boldsymbol{h}_{t-1}$
Output: $\boldsymbol{h}_t$
$\boldsymbol{z}_t \leftarrow \sigma(\text{Linear}_{d_h}(\boldsymbol{x}_t))$
$\tilde{\boldsymbol{h}}_t \leftarrow \text{g}(\text{Linear}_{d_h}(\boldsymbol{x}_t))$
$\boldsymbol{h}_t \leftarrow (\mathbf{1} - \boldsymbol{z}_t) \odot \boldsymbol{h}_{t-1} + \boldsymbol{z}_t \odot \tilde{\boldsymbol{h}}_t$

Algorithm 6 Parallel Mode: Minimal Version of GRU (minGRU) for training in log-space

Input: $\boldsymbol{x}_{1:t}, \boldsymbol{h}_0$
Output: $\boldsymbol{h}_{1:t}$
$\text{linear_z} \leftarrow \text{Linear}_{d_h}$
$\text{log_}\boldsymbol{z}_{1:t} \leftarrow -\text{Softplus}(\text{linear_z}(-\boldsymbol{x}_{1:t}))$
$\text{log_coeffs} \leftarrow -\text{Softplus}(\text{linear_z}(\boldsymbol{x}_{1:t}))$
$\text{log_}\boldsymbol{h}_0 \leftarrow \log(h_0)$
$\text{log_}\tilde{\boldsymbol{h}}_{1:t} \leftarrow \text{log_g}(\text{Linear}_{d_h}(\boldsymbol{x}_{1:t}))$
$\boldsymbol{h}_{1:t} \leftarrow \text{ParallelScanLog}(\text{log_coeffs}, [\text{log_}\boldsymbol{h}_0, \text{log_}\boldsymbol{z}_{1:t} + \text{log_}\tilde{\boldsymbol{h}}_{1:t})$

B.2.2 MINLSTM: A MINIMAL LSTM

We also derive minLSTM's log-space formulation as well. Recall minLSTM's recurrence is as follows $\boldsymbol{h}_t \leftarrow \boldsymbol{f}'_t \odot \boldsymbol{h}_{t-1} + \boldsymbol{i}'_t \odot \tilde{\boldsymbol{h}}_t$. As such, $\boldsymbol{a}_t \leftarrow \boldsymbol{f}'_t$ and $\boldsymbol{b}_t \leftarrow \boldsymbol{i}'_t \odot \tilde{\boldsymbol{h}}_t$. As a result, $\log(\boldsymbol{a}_t) \leftarrow \log(\boldsymbol{f}'_t)$ and $\log(\boldsymbol{b}_t) \leftarrow \log(\boldsymbol{i}'_t) + \log(\tilde{\boldsymbol{h}}_t)$.

$$
\begin{aligned}
\log(\boldsymbol{f}'_t) &= \log\left(\frac{\boldsymbol{f}_t}{\boldsymbol{f}_t + \boldsymbol{i}_t}\right) \\
&= \log\left(\frac{1}{1 + \frac{\boldsymbol{i}_t}{\boldsymbol{f}_t}}\right) \\
&= -\log\left(1 + \frac{\boldsymbol{i}_t}{\boldsymbol{f}_t}\right) \\
&= -\log\left(1 + \exp\left(\log\left(\frac{\boldsymbol{i}_t}{\boldsymbol{f}_t}\right)\right)\right) \\
&= -\text{Softplus}\left(\log\left(\frac{\boldsymbol{i}_t}{\boldsymbol{f}_t}\right)\right) \\
&= -\text{Softplus}\left(\log(\boldsymbol{i}_t) - \log(\boldsymbol{f}_t)\right)
\end{aligned}
$$

Recall that $\boldsymbol{i}_t$ and $\boldsymbol{f}_t$ are computed via sigmoid. In other words, $\boldsymbol{i}_t = \sigma(\boldsymbol{k}_t)$ and $\boldsymbol{f}_t = \sigma(\boldsymbol{p}_t)$ where $\boldsymbol{k}_t = \text{Linear}_{d_h}(\boldsymbol{x}_t)$ and $\boldsymbol{p}_t = \text{Linear}_{d_h}(\boldsymbol{x}_t)$. Furthermore, recall in minGRU's derivation we showed that $\log(\sigma(\boldsymbol{k}_t)) = -\text{Softplus}(-\boldsymbol{k}_t)$ Using this, we can simplify the computation as follows:

$$
\begin{aligned}
\log(\boldsymbol{f}'_t) &= -\text{Softplus}\left(\log(\sigma(\boldsymbol{k}_t)) - \log(\sigma(\boldsymbol{p}_t))\right) \\
&= -\text{Softplus}\left(\text{Softplus}(-\boldsymbol{p}_t) - \text{Softplus}(-\boldsymbol{k}_t)\right)
\end{aligned}
$$

Similarly, we also get that:

$$\log(\boldsymbol{i}'_t) = -\text{Softplus}\left(\text{Softplus}(-\boldsymbol{k}_t) - \text{Softplus}(-\boldsymbol{p}_t)\right)$$

Combining these derivations, we get the parallel mode (Algorithm 8) for efficient training.

Algorithm 7 Sequential Mode: Minimal Version of LSTM (minLSTM) trained in log-space

Input: $\boldsymbol{x}_t, \boldsymbol{h}_{t-1}$
Output: $\boldsymbol{h}_t$
$\boldsymbol{f}_t \leftarrow \sigma(\text{Linear}_{d_h}(\boldsymbol{x}_t))$
$\boldsymbol{i}_t \leftarrow \sigma(\text{Linear}_{d_h}(\boldsymbol{x}_t))$
$\boldsymbol{f}'_t, \boldsymbol{i}'_t \leftarrow \frac{\boldsymbol{f}_t}{\boldsymbol{f}_t+\boldsymbol{i}_t}, \frac{\boldsymbol{i}_t}{\boldsymbol{f}_t+\boldsymbol{i}_t}$
$\tilde{\boldsymbol{h}}_t \leftarrow g(\text{Linear}_{d_h}(\boldsymbol{x}_t))$
$\boldsymbol{h}_t \leftarrow \boldsymbol{f}'_t \odot \boldsymbol{h}_{t-1} + \boldsymbol{i}'_t \odot \tilde{\boldsymbol{h}}_t$

Algorithm 8 Parallel Mode: Minimal Version of LSTM (minLSTM) for training in log-space

Input: $\boldsymbol{x}_{1:t}, \boldsymbol{h}_0$
Output: $\boldsymbol{h}_{1:t}$
$\text{diff} \leftarrow \text{Softplus}(-\text{Linear}_{d_h}(\boldsymbol{x}_{1:t})) - \text{Softplus}(-\text{Linear}_{d_h}(\boldsymbol{x}_{1:t}))$
$\text{log_}\boldsymbol{f}'_{1:t} \leftarrow -\text{Softplus}(\text{diff})$
$\text{log_}\boldsymbol{i}'_{1:t} \leftarrow -\text{Softplus}(-\text{diff})$
$\text{log_}\boldsymbol{h}_0 \leftarrow \log(h_0)$
$\text{log_}\tilde{\boldsymbol{h}}_{1:t} \leftarrow \text{log_g}(\text{Linear}_{d_h}(\boldsymbol{x}_{1:t}))$
$\boldsymbol{h}_{1:t} \leftarrow \text{ParallelScanLog}(\text{log_}\boldsymbol{f}'_{1:t}, [\text{log_}\boldsymbol{h}_0, \text{log_}\boldsymbol{i}'_{1:t} + \text{log_}\tilde{\boldsymbol{h}}_{1:t})$

B.3 PyTorch Code: Log-Space Version

```
def g(x):
    return torch.where(x >= 0, x+0.5, torch.sigmoid(x))
def log_g(x):
    return torch.where(x >= 0, (F.relu(x)+0.5).log(),
                        -F.softplus(-x))
```

Listing 6: The continuous function g ensures that $\tilde{\boldsymbol{h}}_t \leftarrow g(\text{Linear}_{d_h}(x_t))$ is positive.

B.3.1 minGRU: A Minimal GRU

```
    def forward(self, x_t, h_prev):
        # x_t: (batch_size, 1, input_size)
        # h_prev: (batch_size, 1, hidden_size)

        z = torch.sigmoid(self.linear_z(x_t))
        h_tilde = g(self.linear_h(x_t))
        h_t = (1 - z) * h_prev + z * h_tilde
        return h_t
```

Listing 7: Sequential Mode: Minimal Version of GRU (minGRU) trained in log-space

```
    def forward(self, x, h_0):
        # x: (batch_size, seq_len, input_size)
        # h_0: (batch_size, 1, hidden_size)

```

```
        k = self.linear_z(x)
        log_z = -F.softplus(-k)
        log_coeffs = -F.softplus(k)
        log_h_0 = log_g(h_0)
        log_tilde_h = log_g(self.linear_h(x))
        h = parallel_scan_log(log_coeffs,
                torch.cat([log_h_0, log_z + log_tilde_h], dim=1))
        return h
```

Listing 8: Parallel Mode: Minimal Version of GRU (minGRU) for training in log-space

B.3.2 MINLSTM: A MINIMAL LSTM

```
    def forward(self, x_t, h_prev):
        # x_t: (batch_size, 1, input_size)
        # h_prev: (batch_size, 1, hidden_size)

        f_t = torch.sigmoid(self.linear_f(x_t))
        i_t = torch.sigmoid(self.linear_i(x_t))
        tilde_h_t = g(self.linear_h(x_t))
        f_prime_t = f_t / (f_t + i_t)
        i_prime_t = i_t / (f_t + i_t)
        h_t = f_prime_t * h_prev + i_prime_t * tilde_h_t
        return h_t
```

Listing 9: Sequential Mode: Minimal Version of LSTM (minLSTM) trained in log-space

```
    def forward(self, x, h_0):
        # x: (batch_size, seq_len, input_size)
        # h_0: (batch_size, 1, hidden_size)

        diff = F.softplus(-self.linear_f(x))   \
                        - F.softplus(-self.linear_i(x))
        log_f = -F.softplus(diff)
        log_i = -F.softplus(-diff)
        log_h_0 = torch.log(h_0)
        log_tilde_h = log_g(self.linear_h(x))
        h = parallel_scan_log(log_f,
                torch.cat([log_h_0, log_i + log_tilde_h], dim=1))
        return h
```

Listing 10: Parallel Mode: Minimal Version of LSTM (minLSTM) for training in log-space

C Detailed Experiment Setup

In this section, we describe the experiment setup in detail.

C.1 Datasets

Selective Copying. In this task, the model learns to extract data tokens from a sequence while disregarding noise tokens. Following Gu & Dao (2024), we consider a vocabulary of 16 and sequences of length 4096. Each sequence includes 16 randomly placed data tokens. The remainder of the tokens are noise.

Chomsky Hierarchy. In this task, we consider the Chomsky Hierarchy benchmark (Deletang et al., 2023), which includes a variety of formal language tasks that span different levels of the Chomsky hierarchy. Additionally, we include the two additional tasks described in Beck et al. (2024): Majority and Majority Count. Models are trained on tasks whose sequences vary in length up to 40. Evaluation is conducted for task lengths between 40 and 256 to assess the models' ability to generalize.

Long Range Arena. Our experiments on the Long Range Arena benchmark consist of three sequence modelling tasks with sequence lengths from 1024 to 4000, designed to evaluate architectures on long-range modelling:

- **Retrieval:** Based on the ACL Anthology Network (Radev et al., 2009), the task is to classify whether two citations, represented as integer token sequences, are equivalent. Sequences are of length 4000 with two possible classes.
- **ListOps:** An extended version of ListOps (Nangia & Bowman, 2018). The task is to compute the result of a nested mathematical expression in prefix notation. Sequences are of length 2048 with ten possible classes.
- **G-Image:** Based on CIFAR-10 (Krizhevsky, 2009), the task is to predict the class of 32×32 grayscale images (converted from RGB). Sequences are of length 1024 with ten possible classes.

Reinforcement Learning. In this setting, we consider continuous control tasks from the D4RL benchmark (Fu et al., 2020). These tasks based on MuJoCo comprise of three environments with dense rewards: HalfCheetah, Hopper, and Walker. For each environment, three different datasets are considered that have varying level represent varying levels of data quality:

- Medium (M): One million timesteps generated by a policy scoring about one-third of an expert policy's score.
- Medium-Replay (M-R): A replay buffer from an agent trained to perform like the Medium policy.
- Medium-Expert (M-E): One million timesteps from the Medium policy combined with one million from an expert policy.

Following Fu et al. (2020), reported scores are normalized such that 100 represents an expert policy performance.

Language Modelling. In this setting, we consider the Shakespeare dataset, comprising a collection of text data derived from the works of William Shakespeare. The training and testing data consists of $1,003,854$ and $111,540$ tokens respectively.

C.2 Architecture

In our work, the primary goal was to demonstrate that simplified RNN architectures, such as minLSTM and minGRU, can perform comparably to modern state-of-the-art sequence models. To achieve this, we stick with a minimalistic architecture, following standard practices such as residual connections, normalization, and a downprojection layer for the RNN's expanded hidden states. For more

complex tasks like language modeling and Long Range Arena, standard components (convolutional layer and MLP) are added[5].

Selective Copying: No additional components.

Chomsky Hierarchy: (Conv4 $\rightarrow$ minRNN), i.e., a convolutional layer with a kernel size of 4 is applied temporally before the minimal RNN.

Long Range Arena: (Conv4 $\rightarrow$ minRNN $\rightarrow$ MLP)

Language Modelling: (Conv4 $\rightarrow$ minRNN $\rightarrow$ MLP)

Reinforcement Learning: (minRNN $\rightarrow$ MLP)[6]

C.3 Hyperparameters and general experimental details

Selective Copying. For this task, we closely follow the setup of Gu & Dao (2024), training the model for 400k steps with a batch size of 64 and an input dimension of 64. Due to GPU memory constraints, gradient accumulation is applied, where gradients for two batches of size 32 are accumulated before each gradient update and clipped to 1.0. The optimizer used is Adam with a learning rate of 3×10^{-4} alongside early stopping. Each model consists of 3 layers with a dropout rate of 0.1. The minLSTM and minGRU models have an expansion factor of 6. Baseline results are referenced from the Mamba paper.

Long Range Arena. For this benchmark, we closely follow the setup of Beck et al. (2024). For Retrieval, the models consisted of 6 blocks and an embedding dimension of 128 and were trained with a batch size of 64. For ListOps, the models consisted of 8 blocks and an embedding dimension of 128 and were trained with a batch size of 32. For G-Image, the models consisted of 6 blocks and an embedding dimension of 512 and were trained with a batch size of 64. All models were trained for 250k steps using AdamW optimizer with a learning rate of 0.001, weight decay of 0.05, 10% linear warm-up steps, and cosine annealing.

Chomsky Hierarchy. For this benchmark, we closely follow the setup of Beck et al. (2024), training models consisting of two blocks. The models were trained for 500k steps with a batch size of 256 and the AdamW optimizer with a learning rate of 3×10^{-4} and weight decay of 0.01.

Language Modelling. The models are optimized using AdamW with a learning rate of 1×10^{-3}. Each model consists of three layers, a dropout ratio of 0.2, and an embedding dimension of 384. Training is done with 5k steps using a batch size of 64 and evaluated every 25 steps. Gradients are clipped to 0.25. The Transformer is configured with 6 heads. Mamba uses an SSM state expansion factor of 16 and a block expansion factor of 2. Following Mamba, both minLSTM and minGRU utilize an expansion factor of 2 as well.

Reinforcement Learning. We follow the hyperparameter settings outlined by Ota (2024). For Hopper (Medium) and Hopper (Medium-Replay), an embedding dimension of 256 is used, while all other environments utilize an embedding dimension of 128. The learning rate is set to 1×10^{-4} for Hopper (Medium), Hopper (Medium-Replay), and Walker (Medium). For all other environments and datasets, the learning rate is 1×10^{-3}. The models are optimized using AdamW with a weight decay of 1×10^{-4} and a linear warmup for $10,000$ steps. Each model consists of 3 layers and has a dropout ratio of 0.1. The models are trained for 100k steps with a batch size of 64. Results for the baselines are referenced from the Mamba and Aaren papers.

[5]There is a trend in modern recurrent sequence models of prepending a convolutional layer (kernel size of 4) before their recurrent unit – for example, see Mamba (Gu & Dao, 2024) and xLSTM (Beck et al., 2024) Empirically, we found that including this convolutional layer also helped minRNNs.

[6]Note this is equivalent to the standard Decision Transformer framework for (Offline) RL, replacing the self-attention module with minLSTM or minGRU.

D Additional Experiments

D.1 Chomsky Hierarchy + Long Range Arena

In this section, we conduct experiments on both the Chomsky Hierarchy (Deletang et al., 2023) and Long Range Arena (Tay et al., 2021) benchmarks, which are well-established in the literature for evaluating sequence models. Together, these benchmarks provide a test of a model's ability to generalize and handle long-range dependencies, which are crucial for modern sequence modelling tasks.

We compare Minimal RNNs against other fully parallelizable models, such as RWKV, Mamba, and xLSTM[1:0] (using its parallelizable mLSTM module). Following Beck et al. (2024), we focus on tasks from the Chomsky Hierarchy where models have achieved at least 30% accuracy, indicating partial solvability. We closely followed the hyperparameter configurations outlined in the xLSTM paper and averaged results over 3 seeds for consistency. The baseline results (accuracy – higher is better) are taken from the xLSTM paper (Figure 4 for Chomsky Hierarchy and Table 6 for Long Range Arena).

Our experiments (Table 4 and extended Table 5) show that Minimal RNNs achieve competitive performance with state-of-the-art models (e.g., Mamba and xLSTM) across all tasks on these benchmarks, outperforming other models such as Retention, Hyena, RWKV, and Llama.

D.2 Inference Runtime Comparison

In these experiments, we compare the inference speeds of GRU, LSTM, minGRU, minLSTM, and Mamba (using the official implementation). It is important to note that inference speed may vary depending on the hardware and implementation used.

For this analysis, we tested different batch sizes (8, 16, 32, 64) and sequence lengths (up to 2048). In Figure 3, we present the average inference speed across 50 runs, taking context tokens into account before performing inference. Since GRU and LSTM models process context tokens sequentially, their inference times are considerably slower than those of minGRU, minLSTM, and Mamba, all of which benefit from parallel processing.

Overall, minLSTM and minGRU show inference speeds comparable to Mamba. Specifically, minGRU was 6.6%, 4.1%, 4.9%, and 2.9% faster than Mamba for batch sizes of 8, 16, 32, and 64, respectively. On the other hand, minLSTM was 3.6%, 2.9%, 0%, and 1.3% slower than Mamba for the same batch sizes.

Since minLSTM and minGRU are simplifications of LSTM and GRU, we expect them to generally perform faster, including during inference. This is demonstrated in Figure 4, where we compare the inference speed of minLSTM and minGRU with traditional LSTM and GRU models across varying batch sizes. As expected, minGRU and minLSTM are 19.6% and 41.5% faster than GRU and LSTM for a batch size of 64, respectively.

D.3 Architecture Ablation

In our work, the main objective was to demonstrate that simplified RNN architectures, such as minLSTM and minGRU, can perform on par with modern state-of-the-art sequence models. To achieve this, we adopted a minimalistic architectural design, incorporating standard practices such as residual connections, normalization, and a downprojection layer for the RNN's expanded hidden states. For more complex tasks, like language modeling and Long Range Arena, we introduced a convolutional layer and a multi-layer perceptron (MLP).

To better understand the impact of these architectural choices, we conducted an ablation study on the ListOps (Long Range Arena) dataset of these additional components. The results, averaged over 3 seeds, are shown in Table 6. The table highlights the effect of adding different layers to the minLSTM model. For ListOps, incorporating a convolutional layer (Conv) and an MLP resulted in improved performance.

Method		Bucket Sort	Missing Duplicate	Cycle Nav.	Even Pairs	Majority
Transformers	Llama	0.92	0.08	0.04	1.0	0.37
Modern RNNs	Mamba	0.69	0.15	0.86	1.0	0.69
	RWKV-4	0.54	0.21	0.13	1.0	0.63
	xLSTM	0.97	0.33	0.86	1.0	0.74
Minimal RNNs	minLSTM (Ours)	0.94	0.26	0.79	1.0	0.93

Method		Majority Count	Retrieval	ListOps	G-Image	Average
Transformers	Llama	0.13	0.85	0.38	0.54	0.48
Modern RNNs	Mamba	0.45	0.90	0.33	0.69	0.64
	RWKV-4	0.13	0.90	0.39	0.69	0.51
	xLSTM	0.46	0.91	0.41	0.70	0.71
Minimal RNNs	minLSTM (Ours)	0.47	0.89	0.59	0.67	0.73

Table 4: **Results for Chomsky Hierarchy and Long Range Arena Benchmarks.** We compare minLSTM against other fully parallelizable models, including RWKV, Mamba, and xLSTM[1:0] (using the mLSTM module). The baseline results (accuracy – higher is better) are taken from the xLSTM paper (Figure 4 for Chomsky Hierarchy and Table 6 for Long Range Arena). The results demonstrate that minLSTM achieves competitive performance with state-of-the-art models such as Mamba and xLSTM across all tasks on these benchmarks.

D.4 Initialization Analyses

In this set of experiments, we examine the effect of initialization on the model's performance. Depending on the task at hand, it may be beneficial to encourage the model to retain information over time. One way to achieve this is by increasing the bias term in the forget gate of the minLSTM, which promotes information retention earlier in the training process. As a result, the forget gate f_t of the LSTM approaches a value of 1 due to this new initialization. As shown in Figure 5, increasing the forget gate bias in minLSTM enhances training efficiency, leading to faster convergence and greater stability during training.

E Additional Related Work

Parallel Scan. Generalizing across the families of methods (including minLSTM and minGRU), these recent sequence models can be viewed as members of the same family of functions trainable via a parallel scan: $\boldsymbol{v}_t = \boldsymbol{a}_t \odot \boldsymbol{v}_{t-1} + \boldsymbol{b}_t$ (see Section 2.3) where $\boldsymbol{a}_t$ and $\boldsymbol{b}_t$ are functions of the input token $\boldsymbol{x}_t$. Improving upon the parallel scan algorithm, several models (Yang et al., 2024; Gu & Dao, 2024) such as Mamba have proposed specialized hardware-efficient methods that leverage GPU's memory hierarchy to reduce high I/O costs and speed up training. In our work, we implemented minLSTM and minGRU in plain PyTorch. However, due to the structural similarities in recurrences amongst the numerous methods that leverage parallel scan, many techniques such as chunking that apply to one work for speeding up training can also apply to others such as minGRU and minLSTM.

Parameter Initializations. Unrolling the recurrences of these new recurrent sequence models over time often results in their outputs and gradients vanishing/exploding (Wang et al., 2024) due to time dependency in their output's scale. To ensure model stability, the parameters of many models such as state-space models are initialized according to special distributions (Gu et al., 2020; 2022; Orvieto et al., 2023). In contrast, we found that minLSTM and minGRU are already stable using the default PyTorch initialization. Unlike SSMs, minLSTM and minGRU's outputs are time-independent in scale, avoiding potential instabilities.

Method		Context Sensitive		Regular		xLSTM	
		Bucket Sort	Missing Duplicate	Cycle Nav.	Even Pairs	Majority	Majority Count
Traditional RNNs	GRU	0.54	0.29	0.94	1.0	0.60	0.42
	LSTM	0.99	0.33	1.0	1.0	0.54	0.46
Transformers	Llama	0.92	0.08	0.04	1.0	0.37	0.13
Modern RNNs	Mamba	0.69	0.15	0.86	1.0	0.69	0.45
	Retention	0.13	0.03	0.05	0.51	0.36	0.12
	Hyena	0.3	0.06	0.06	0.93	0.36	0.18
	RWKV-4	0.54	0.21	0.13	1.0	0.63	0.13
	RWKV-5	0.49	0.15	0.26	1.0	0.73	0.34
	RWKV-6	0.96	0.23	0.31	1.0	0.76	0.24
	xLSTM	0.97	0.33	0.86	1.0	0.74	0.46
Minimal RNNs	minLSTM (Ours)	0.94	0.26	0.79	1.0	0.93	0.47

Table 5: **Extended Results for Chomsky Hierarchy Benchmark.** The baseline results (accuracy — higher is better) are taken from the xLSTM paper (Figure 4). We compare minLSTM against other fully parallelizable models, including RWKV, Mamba, and xLSTM[1:0] (using the mLSTM module). The results demonstrate that minLSTM achieves competitive performance with state-of-the-art models such as Mamba and xLSTM, while outperforming other models like Retention, Hyena, RWKV, and Llama across all tasks in the Chomsky Hierarchy benchmark.

Model	Accuracy
minLSTM	0.46
minLSTM (+ Conv)	0.45
minLSTM (+ MLP)	0.52
minLSTM (+ Conv + MLP)	0.59

Table 6: **Architecture Ablation on the ListOps (Long Range Arena) Dataset.** Results (accuracy – higher is better) are averaged over 3 seeds. The table shows the impact of adding different layers to the minLSTM model. For more complex tasks like language modeling and Long Range Arena, we incorporate a convolutional layer (Conv) and a multi-layer perceptron (MLP). The performance increases when these components are added.

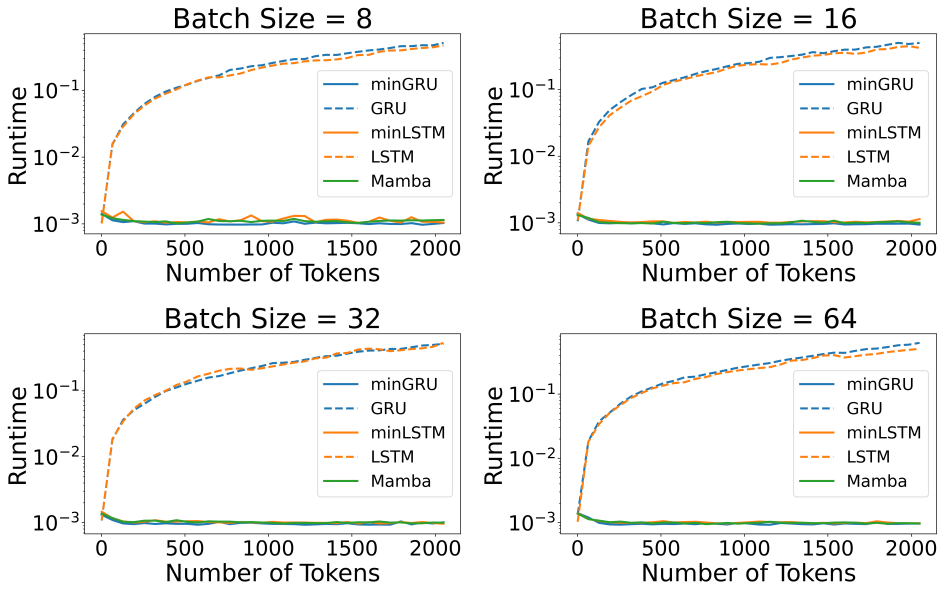

Figure 3: **Runtime Comparison of Inference with Context Tokens: Parallelizable RNNs (minLSTM, minGRU, and Mamba) vs. Traditional RNNs (LSTM and GRU).** As sequential models, LSTM and GRU exhibit significantly slower inference times when processing an increasing number of context tokens, compared to the parallelizable models minLSTM, minGRU, and Mamba.

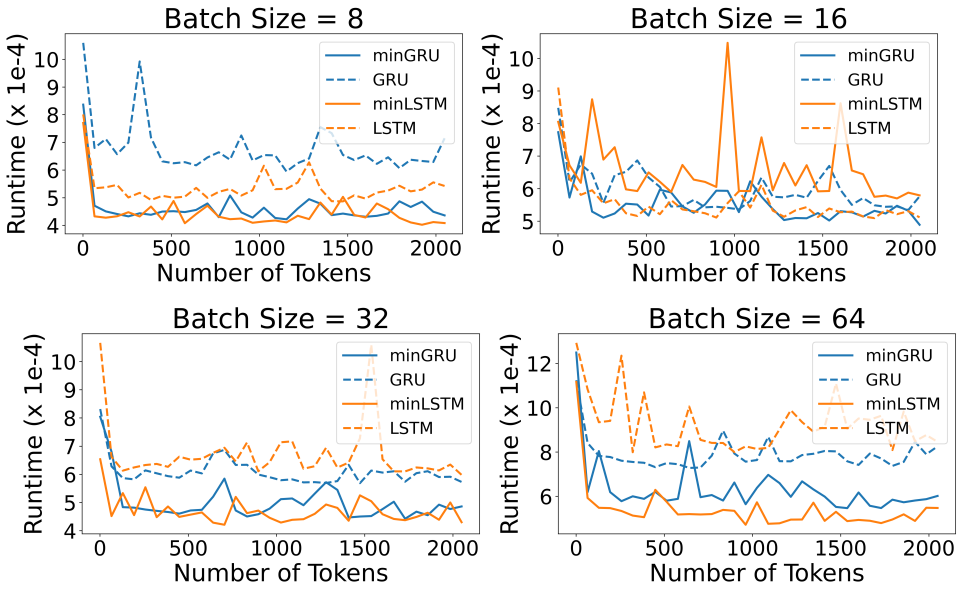

Figure 4: **Runtime Comparison of Inference: Minimal RNNs (minLSTM and minGRU) vs. Traditional Counterparts (LSTM and GRU).** As simplified versions of LSTM and GRU, minLSTM and minGRU generally exhibit faster inference times, particularly with larger batch sizes, as shown in the plots.

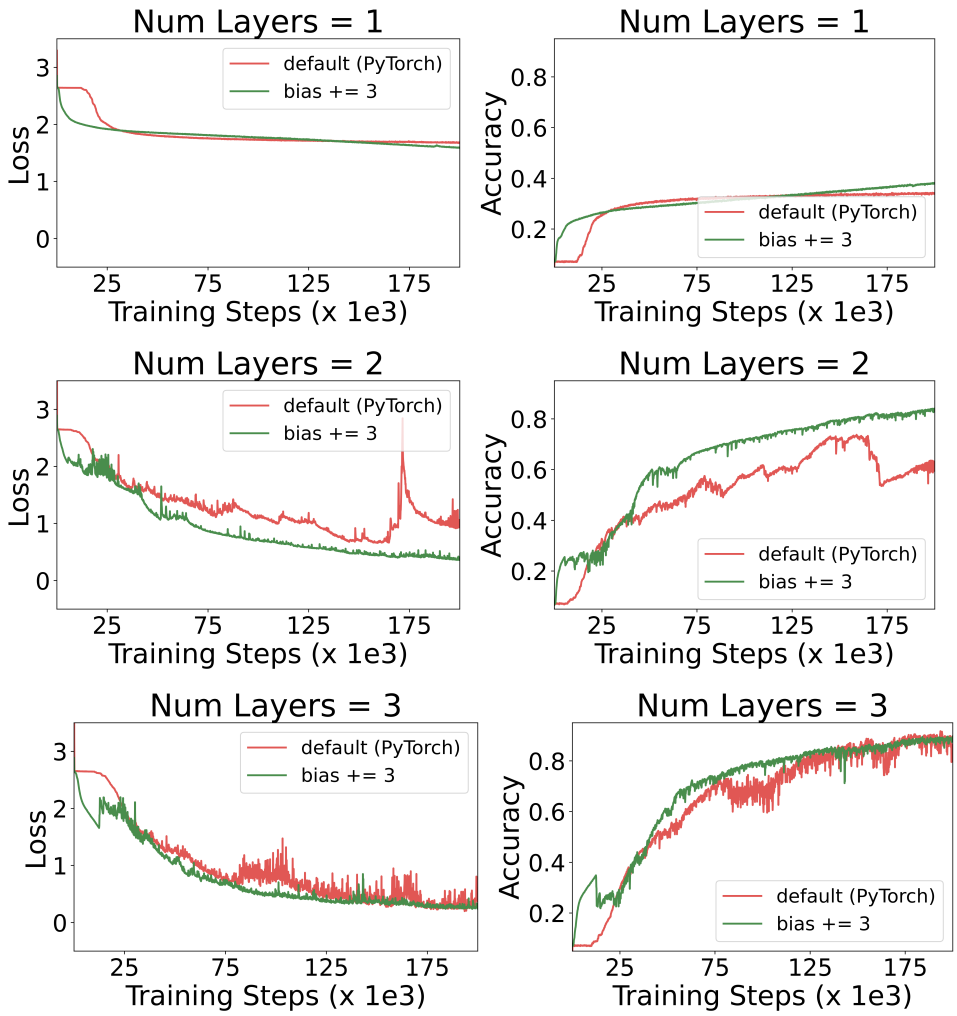

Figure 5: **Impact of Forget Gate Bias Initialization on Training Efficiency.** The plot illustrates how increasing the bias of the forget gate in minLSTM enhances training efficiency by promoting earlier retention of information, leading to faster convergence and a more stable training process.